Electrodes controlling phase diagrams of symmetric ferroelectric tunneling junctions or capacitors

W. J. Chen, Yue Zheng, and Biao Wang

Citation: Appl. Phys. Lett. **98**, 222902 (2011); doi: 10.1063/1.3591163
View online: http://dx.doi.org/10.1063/1.3591163
View Table of Contents: http://aip.scitation.org/toc/apl/98/22
Published by the American Institute of Physics

Electrodes controlling phase diagrams of symmetric ferroelectric tunneling junctions or capacitors

W. J. Chen, Yue Zheng,[a] and Biao Wang[a]
State Key Laboratory of Optoelectronic Materials and Technologies, School of Physics and Engineering, Sun Yat-sen University, 510275 Guangzhou, People's Republic of China

(Received 5 January 2011; accepted 6 April 2011; published online 2 June 2011)

Electrodes controlling the "misfit strain-temperature" phase diagrams of symmetric ferroelectric tunneling junctions or capacitors have been investigated. Taking into account effect of the imperfect charge screening in electrodes, it is found that the phase diagrams can be significantly shifted with changing coefficients of electrodes. Results about the dielectric constants also indicate promising controllability of other properties for ferroelectric tunnel junction or capacitor by adjusting electrodes. © *2011 American Institute of Physics*. [doi:10.1063/1.3591163]

Nanoscale electrode-ferroelectric-electrode heterostructures, such as ferroelectric tunnel junction (FTJ) and ferroelectric capacitor (FC), have shown important electronic properties.[1–5] It is well known that properties of FTJ or FC can be significantly affected by many factors, such as thickness, surface and interface, etc.[6–10] According to recent works, critical properties of FTJ and FC are also obviously affected by properties of electrodes. For example, a critical thickness has been found in $SrRuO_3/BaTiO_3/SrRuO_3$ capacitor. The depolarization field due to the imperfect charge screening in electrodes was summarized as a main reason to suppress ferroelectricity.[11] Similarly, Umeno *et al.*[12] investigated the spontaneous polarization in the $Pt/PbTiO_3/Pt$ capacitor, and demonstrated that the critical thickness exists due to effect of the charge screening in electrodes. More importantly, Kim *et al.*[13] demonstrated stability of the spontaneous polarization can be determined by properties of electrodes. Zheng *et al.*[14] derived analytic expressions about the critical properties as functions of coefficients of electrodes.

For $BaTiO_3$ and $PbTiO_3$ single-domain thin films epitaxially grown on substrates, the "misfit strain-temperature" (MST) phase diagrams have been constructed.[15] Subsequently, Morozovska *et al.*[16] gave analytical expressions of the phase diagram for a ferroelectric thin film (FTF). Using the phase field simulations, the phase diagrams as function of the FTF thickness have also been investigated.[17,18] Up to now, a systematic investigation of electrodes effect on the MST phase diagrams of FTJ or FC has not yet been given. In this paper, we report electrodes controlling the MST phase diagrams of FTJ or FC. With changing electrodes, it is found that the MST phase diagrams as well as the dielectric property of FTJ or FC can be significantly affected as function of coefficients of electrodes.

We consider a configuration of a symmetric FTJ or FC with a single-domain ABO_3-type FTF of thicknesses h sandwiched by electrodes each of thickness $L/2$ (see Fig. 1). Under the short-circuit boundary condition, compensation charges with screening length l_e are induced in the electrodes. The spontaneous polarization $\mathbf{P}=(P_1,P_2,P_3)$ is defined as polarization from the permanent electric moment. Therefore, the electric displacement field $\mathbf{D}$ at constant applied stress and temperature can be expressed in terms of the linear-part induced polarization $\mathbf{P^E}$ and nonlinear-part spontaneous polarization $\mathbf{P}$ as $\mathbf{D}=\varepsilon_0\mathbf{E}+\mathbf{P^E}+\mathbf{P}=\varepsilon_0\mathbf{E}+\boldsymbol{\chi}_\mathbf{b}\mathbf{E}+\mathbf{P}=\boldsymbol{\varepsilon}_\mathbf{b}\mathbf{E}+\mathbf{P}$, where $\boldsymbol{\chi}_\mathbf{b}$ and $\boldsymbol{\varepsilon}_\mathbf{b}$ are the background susceptibility and dielectric constant tensor of the background materials.[19,20] Since the background material is the paraelectric phase, which is a cubic crystal structure, and the background dielectric constants in three axis directions are the same, i.e., $\varepsilon_b=\varepsilon_{11b}=\varepsilon_{22b}=\varepsilon_{33b}$.

Taking into account effects of mechanical stresses, surfaces, and electric fields, the total free energy of the ferroelectric materials in nanoscale can be given as sum of bulk free energy, elastic energy, electric energy, and surface energy. For a FTF epitaxially grown on substrate, the sum of its bulk free energy density f_{bulk} and elastic energy density f_{elastic} can be given by,[15,18,21–24]

$$\begin{aligned} f_{\text{bulk}}+f_{\text{elastic}} &= \alpha_1^*(P_1^2+P_2^2)+\alpha_3^*P_3^2+\alpha_{11}^*(P_1^4+P_2^4) \\ &+\alpha_{33}^*P_3^4+\alpha_{13}^*(P_1^2+P_2^2)P_3^2+\alpha_{12}^*P_1^2P_2^2 \\ &+\alpha_{112}[P_1^4(P_2^2+P_3^2)+P_2^4(P_1^2+P_3^2)+P_3^4(P_1^2 \\ &+P_2^2)]+\alpha_{111}(P_1^6+P_2^6+P_3^6)+\alpha_{123}P_1^2P_2^2P_3^2 \end{aligned}$$

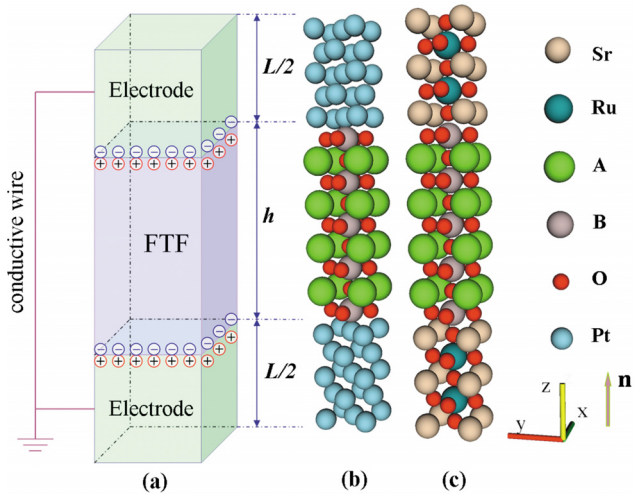

FIG. 1. (Color online) (a) Schematic configuration of a typical FTJ with the short-circuit boundary condition. Atomic structures of FTJ with (b) Pt and (c) $SrRuO_3$ symmetric electrodes, respectively.

[a]Authors to whom correspondence should be addressed. Electronic addresses: zhengy35@mail.sysu.edu.cn and wangbiao@mail.sysu.edu.cn.

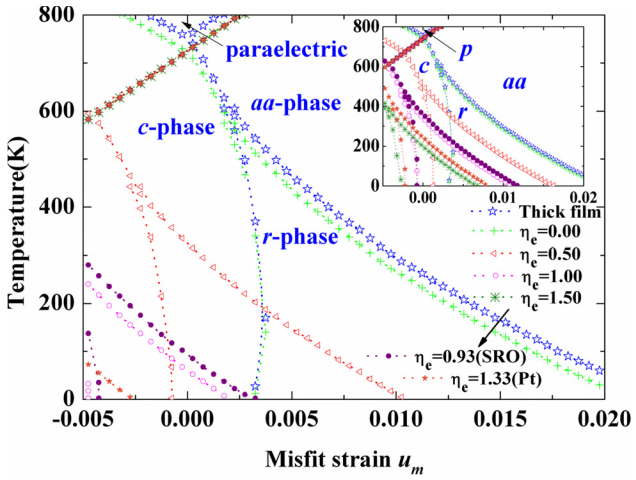

FIG. 2. (Color online) Phase diagrams of $PbTiO_3$ FTJ or FC of thicknesses 10nm and 20nm (inserted figure) with various electrodes.

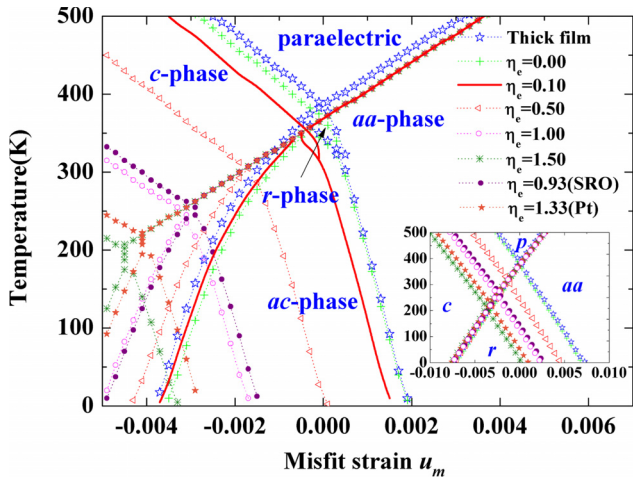

FIG. 3. (Color online) Phase diagrams of 20–nm-thick $BaTiO_3$ FTJ or FC with various electrodes. The inserted figure depicts those obtained using the eight-order approximated potential.

$$+ (s_{11} + s_{12})^{-1} u_m^2, \tag{1}$$

where the dielectric stiffness $\alpha_1 \equiv (T - T_{c0})/(2\varepsilon_0 C_0)$ and the second order stiffness coefficients α_{ij} at constant stress have been renormalized into α_i^* and α_{ij}^* by the misfit strain u_m,[15,18,25] and α_{ijk} are higher order stiffness coefficients; s_{ij} and Q_{ij} are the elastic compliance coefficients and electrostrictive coefficients, respectively. Note that u_m should be considered as the thickness-dependent effective misfit strain with appearance of the interfacial dislocations for a thick film epitaxially grown on substrate[10] because the misfit strain relaxation would happen for the film thickness above a critical thickness of the interfacial dislocation generation.

For a FTJ or FC, we assume that the x and y dimensions are infinite, so we only consider the depolarization field along the z direction. In the absence of external electric field, the internal electric field is equal to the depolarization field and can be expressed as $E_d = -\varepsilon_b^{-1}(1-\theta)P_3$ with $\theta \equiv h\varepsilon_b^{-1}(2l_e\varepsilon_e^{-1} + h\varepsilon_b^{-1})^{-1}$, where ε_e is the dielectric constant of electrode.[13,14] It can be seen that the depolarization field is determined by ratio of the screening length and the dielectric constant, i.e., $\eta_e = l_e\varepsilon_e^{-1}$, for the FTF with a fixed thickness. Using Landau and Lifshitz functional,[21] the electric energy density f_{elec} should be expressed as $f_{\text{elec}} = -P_3E_d - (1/2)\varepsilon_b E_d^2$.

The surface contribution to the energy should be considered, which contains the effect of any near-interface variation in polarization and describes the direct coupling between the polarization and interface. In this letter, we define this energy as the surface energy, which can be written as a Taylor expansion.[22] Retaining the two lowest terms of the Taylor expansion, the surface energy density f_{surf} for a FTJ or FC is approximately given by $f_{\text{surf}} = (\zeta_{1i} - \zeta_{2i})P_i + (\eta_{1i} + \eta_{2i})P_i^2/2$, where coefficients of the surface energy expansion for the two FTF surfaces are denoted as ζ_{1i}, η_{1i}, and ζ_{2i}, η_{2i} with respect to P_i, respectively. In case of symmetric electrodes and interfaces, we set $\zeta_{1i} = \zeta_{2i} = \zeta$ and $\eta_{1i} = \eta_{2i} = \eta$ in present letter.

From what has been discussed above, the total free energy of a symmetric FTJ or FC is contributed from f_{bulk}, f_{elastic}, f_{elec}, and f_{surf} and can be given by,

$$\begin{aligned} F = Sh\{&\alpha_1^*(P_1^2 + P_2^2) + \alpha_3^* P_3^2 + \alpha_{11}^*(P_1^4 + P_2^4) + \alpha_{33}^* P_3^4 \\ &+ \alpha_{13}^*(P_1^2 + P_2^2)P_3^2 + \alpha_{12}^* P_1^2 P_2^2 + \alpha_{112}[P_1^4(P_2^2 + P_3^2) \\ &+ P_2^4(P_1^2 + P_3^2) + P_3^4(P_1^2 + P_2^2)] + \alpha_{111}(P_1^6 + P_2^6 + P_3^6) \\ &+ \alpha_{123} P_1^2 P_2^2 P_3^2 + (s_{11} + s_{12})^{-1} u_m^2 + \xi_d P_3^2/2\} + S\eta(P_1^2 \\ &+ P_2^2 + P_3^2), \end{aligned} \tag{2}$$

where S represents the area of the upper or lower surface plane of FTF. ξ_d reflects the effect of depolarization field and can be written as $\xi_d = \varepsilon_b^{-1}(1-\theta^2)$. Minimization of the total free energy with respect to the polarization components, the equilibrium spontaneous polarizations can be solved by the following equations, i.e., $\partial F/\partial P_i = 0$.

As can be seen from Eq. (2), the second-order coefficients of the free energy expression are renormalized by the surface effect and depolarization field. According to Pertsev and co-workers,[23] we introduce the effective temperature $\tilde{T}$ and effective misfit strain $\tilde{u}_m$ so that the second-order coefficients can be written as $\alpha_1^*(T, u_m) + \eta/h = \alpha_1^*(\tilde{T}, \tilde{u}_m)$ and $\alpha_3^*(T, u_m) + \xi_d/2 + \eta/h = \alpha_3^*(\tilde{T}, \tilde{u}_m)$. If other coefficients of the free energy expression are independent of temperature and the misfit strain, such as the six-order approximated free energy expression for $PbTiO_3$ (Ref. 15) and the eight-order approximated one for $BaTiO_3$,[24] we can derive temperature and the misfit strain shift of the MST phase diagram due to the depolarization field and surface effects, i.e., $\Delta T = 2\varepsilon_0 C_0[\xi_d(Q_{11} + Q_{12})(Q_{12} - Q_{11})^{-1}/2 - \eta h^{-1}]$ and $\Delta u_m = \xi_d(s_{11} + s_{12})(Q_{12} - Q_{11})^{-1}/2$, where $\Delta T \equiv T - \tilde{T}$ and $\Delta u_m \equiv u_m - \tilde{u}_m$.[25] However, this construction of the MST phase diagram does not work for the six-order approximated free energy expression of $BaTiO_3$ (Ref. 15) since α_{11} and α_{113} are also temperature-dependent.

In following calculations, we consider $PbTiO_3$ and $BaTiO_3$ FTFs sandwiched between symmetric electrodes, i.e., $SrRuO_3$ and Pt, etc. Values of expansion coefficients of the six-order approximated potential for $PbTiO_3$ and $BaTiO_3$, including electrostrictive coefficients and elastic compliance coefficients are from Ref. 15. Those of the eight-order approximated potential for $BaTiO_3$ can be found in Ref. 24. For $SrRuO_3$ and Pt electrodes, ratio of the dielectric constant and screening length η_e are taken as 0.93 F^{-1} m^2 and 1.33 F^{-1} m^2, respectively.[3] The background dielectric constant and coefficient about surface effect are listed as $\varepsilon_b \approx 50\varepsilon_0$ (Ref. 14) and $\varepsilon_0\eta \approx 0.01 \times 10^{-10}$ m.[22]

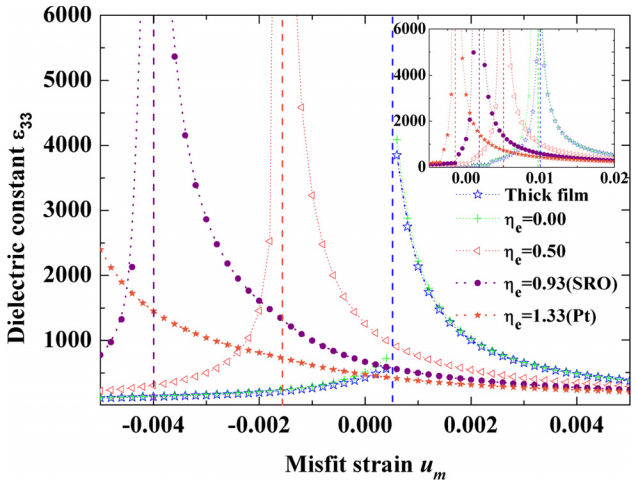

FIG. 4. (Color online) Dielectric constant ε_{33} of 20-nm-thick $BaTiO_3$ and $PbTiO_3$ (inserted figure) FTJ or FC with various electrodes at $T=300$ K.

Effects of electrodes on MST phase diagrams of 10-nm-thick and 20-nm-thick $PbTiO_3$ thin film are shown in Fig. 2 and inserted figure therein, respectively, where $\eta_e=0$ means the perfect charge screening and the depolarization field can be neglected. In order to have a comparison, MST phase diagram of a relative thick film (i.e., $h=100$ nm) on which the size effects are negligible, is also plotted. It can be seen that the surface effect shifts the whole MST phase diagram to lower temperature. Taking into account effect of the depolarization field, Fig. 2 also shows that the whole phase diagram in is shifted along the transition line between the paraelectric phase and *aa*-phase to lower temperature and more negative misfit strain, and indicates that larger η_e makes the in-plane polarization state, i.e., *aa*-phase, more energetic favor. Comparing Fig. 2 with the inserted figure, we can also find that electrode changing induces more significant shifts of the MST phase diagram in thinner FTF. We would like to compare the effects of the depolarization field due to imperfect charge screening and that induced by a finite gap between the FTF and ideal electrode.[10] For a 10-nm-thick $PbTiO_3$ FTF, the Curie temperature of the out-of-plane polarization due to the imperfect charge screening is estimated to be lowered by $\xi_d\varepsilon_0 C_0$ [see Eq. (2)], e.g., ~435 K for $SrRuO_3$ electrodes and ~593 K for Pt electrodes, which is comparable with shift of the Curie temperature caused by a 0.5 Å vacuum gap in Morozovska *et al.*'s work.[10]

Using a six-order approximated potential, similar shifts of the MST phase diagrams of 20–nm-thick $BaTiO_3$ FTFs are also observed as shown in Fig. 3. However, different from the whole shifts of phase diagrams of $PbTiO_3$ FTFs without changing the relative positions of the transition lines, Fig. 3 shows that *r*-phase of $BaTiO_3$ FTFs obviously shrinks with η_e increasing, and disappears in the whole range of temperature and misfit strain as $\eta_e>0.2$. This shrinking of *r*-phase is due to the temperature-dependent and α_{11} and α_{113} in six-order approximated potential. More significant shifts of the MST phase diagram in thinner α_{113} are also observed. Using the eight-order approximated potential, the inserted figure in Fig. 3 depicts the phase diagrams of 20–nm-thick $BaTiO_3$ FTF.

Influences of electrodes changing on the dielectric constant ε_{33} $T=300$ K are shown in Fig 4 and the inserted figure for 20-nm-thick $BaTiO_3$ and $PbTiO_3$ FTFs, respectively. It can be seen that the phase transition temperature obviously shifts to the lower temperature with η_e increasing and the dielectric constants are very sensitive to coefficient η_e of electrodes. Similar behaviors of electrode controlling other dielectric constants of FTJ or FC are also observed.

In summary, we have investigated electrodes controlling the MST phase diagrams of symmetric FTJ or FC. It is found that significant shifts of the MST phase diagrams can be obtained with coefficients of electrodes changing, i.e., ratio of the screening length and dielectric constant. Results about the dielectric constants also indicate promising controllability of other properties by adjusting electrodes.

This project is grateful for support from the NSFC (Nos. 10902128, 10732100, 11072271, 10972239), the FRF for the Central Universities.

[1]M. Y. Zhuravlev, R. F. Sabirianov, S. S. Jaswal, and E. Y. Tsymbal, Phys. Rev. Lett. **94**, 246802 (2005).
[2]E. Y. Tsymbal and H. Kohlstedt, Science **313**, 181 (2006).
[3]Y. Zheng and C. H. Woo, Nanotechnology **20**, 075401 (2009).
[4]X. Luo, B. Wang, and Y. Zheng, ACS Nano **5**, 1649 (2011).
[5]V. Garcia, S. Fusil, K. Bouzehouane, S. E. Vedrenne, N. D. Mathur, A. Barthelemy, and M. Bibes, Nature (London) **460**, 81 (2009).
[6]A. V. Bune, V. M. Fridkin, S. Ducharme, L. M. Blinov, S. P. Palto, A. V. Sorokin, S. G. Yudin, and A. Zlatkin, Nature (London) **391**, 874 (1998).
[7]D. D. Fong, G. B. Stephenson, S. K. Streiffer, J. A. Eastman, O. Auciello, P. H. Fuoss, and C. Thompson, Science **304**, 1650 (2004).
[8]D. D. Fong, A. M. Kolpak, J. A. Eastman, S. K. Streiffer, P. H. Fuoss, G. B. Stephenson, C. Thompson, D. M. Kim, K. J. Choi, C. B. Eom, I. Grinberg, and A. M. Rappe, Phys. Rev. Lett. **96**, 127601 (2006).
[9]D. A. Tenne, P. Turner, J. D. Schmidt, M. Biegalski, Y. L. Li, L. Q. Chen, A. Soukiassian, S. Trolier-McKinstry, D. G. Schlom, X. X. Xi, D. D. Fong, P. H. Fuoss, J. A. Eastman, G. B. Stephenson, C. Thompson, and S. K. Streiffer, Phys. Rev. Lett. **103**, 177601 (2009).
[10]A. N. Morozovska, E. A. Eliseev, S. V. Svechnikov, A. D. Krutov, V. Y. Shur, A. Y. Borisevich, P. Maksymovych, and S. V. Kalinin, Phys. Rev. B **81**, 205308 (2010).
[11]J. Junquera and P. Ghosez, Nature (London) **422**, 506 (2003).
[12]Y. Umeno, B. Meyer, C. Elsässer, and P. Gumbsch, Phys. Rev. B **74**, 060101(R) (2006).
[13]D. J. Kim, J. Y. Jo, Y. S. Kim, Y. J. Chang, J. S. Lee, T. K. Jong-Gul, Y. Song, and T. W. Noh, Phys. Rev. Lett. **95**, 237602 (2005).
[14]Y. Zheng, M. Q. Cai, and C. H. Woo, Acta Mater. **58**, 3050 (2010).
[15]N. A. Pertsev, A. G. Zembilgotov, and A. K. Tagantsev, Phys. Rev. Lett. **80**, 1988 (1998).
[16]M. D. Glinchuk, A. N. Morozovska, and E. A. Eliseev, J. Appl. Phys. **99**, 114102 (2006).
[17]Y. L. Li, S. Y. Hu, Z. K. Liu, and L. Q. Chen, Appl. Phys. Lett. **78**, 3878 (2001).
[18]D. C. Ma, Y. Zheng, and C. H. Woo, Appl. Phys. Lett. **95**, 262901 (2009).
[19]Y. Zheng and C. H. Woo, Appl. Phys. A: Mater. Sci. Process. **97**, 617 (2009); C. H. Woo and Y. Zheng, *ibid.* **91**, 59 (2008).
[20]A. K. Tagantsev, Ferroelectrics **375**, 19 (2008).
[21]L. D. Landau, E. M. Lifshitz, and L. P. Pitaevskii, *Electrodynamics of Continuous Media*, 1st ed. (Oxford University Press, New York, 1960); *Electrodynamics of Continuous Media*, 2nd ed. (Oxford University Press, New York, 1984).
[22]G. Gerra, A. K. Tagantsev, and N. Setter, Phys. Rev. Lett. **98**, 207601 (2007); A. K. Tagantsev, G. Gerra, and N. Setter, Phys. Rev. B **77**, 174111 (2008).
[23]F. A. Urtiev, V. G. Kukhar, and N. A. Pertsev, Appl. Phys. Lett. **90**, 252910 (2007).
[24]Y. L. Li, L. E. Cross, and L. Q. Chen, J. Appl. Phys. **98**, 064101 (2005).
[25]See supplementary material at http://dx.doi.org/10.1063/1.3591163 for providing the derivation of temperature and the misfit strain shift of the MST phase diagram.